Axial Liquid Mixing in High-Pressure Bubble Columns

G. Q. Yang and L. S. Fan
Dept. of Chemical Engineering, The Ohio State University, Columbus, OH 43210

Axial dispersion coefficients of the liquid phase in bubble columns at high pressure are investigated using the thermal dispersion technique. Water and hydrocarbon liquids are used as the liquid phase. The system pressure varies up to 10.3 MPa and the superficial gas velocity varies up to 0.4 cm/s, which covers both the homogeneous bubbling and churn-turbulent flow regimes. Experimental results show that flow regime, system pressure, liquid properties, liquid-phase motion, and column size are the main factors affecting liquid mixing. The axial dispersion coefficient of the liquid phase increases with an increase in gas velocity and decreases with increasing pressure. The effects of gas velocity and pressure on liquid mixing can be explained based on the combined mechanism of global liquid internal circulation and local turbulent fluctuations. The axial liquid dispersion coefficient also increases with increasing liquid velocity due to enhanced liquid-phase turbulence. The scale-up effect on liquid mixing reduces as the pressure increases.

Introduction

Bubble column and slurry bubble column reactors operating at high pressures are commonly encountered in many industrial processes such as methanol synthesis, resid hydrotreating, Fischer-Tropsch synthesis, and benzene hydrogenation. One feature of bubble column reactors is the nonideal flow pattern of each individual phase, which significantly influences reactant conversion and selectivity. In bubble columns, the dispersed gas phase moves in a continuous liquid medium, and, thus, the mixing behavior of the liquid phase is mainly affected by the agitating action of rising bubbles. Many studies have shown that pressure has a significant effect on bubble characteristics. Therefore, study of the effect of pressure on liquid mixing behavior is necessary for the design of industrial reactors.

Studies regarding the axial liquid-phase mixing in bubble columns at atmospheric conditions are extensive, especially for the air-water system; however, studies under high-pressure conditions are very scarce. Houzelot et al. (1985) investigated the axial dispersion behavior of the liquid phase in a bubble column with a diameter of 5 cm and a height of 4 m. An insignificant effect of pressure on the axial dispersion was observed, which was limited by the narrow experimental conditions in their study, that is, very low superficial gas velocity (< 6 mm/s) and pressure (< 3 atm). Under such conditions, the flow is always in the homogeneous bubbling regime and a significant change in liquid-phase mixing within such narrow operating conditions is not expected. Sangnimnuan et al. (1984) experimentally investigated the extent of liquid-phase backmixing under industrial coal hydroliquefaction conditions (temperature between 164 and 384°C and pressure between 4.5 and 15 MPa) in a small bubble column reactor (1.9 cm in diameter and 222 cm in height). They did not describe the effect of pressure on axial mixing and their study was limited by the small size of the reactor.

Holcombe et al. (1983) determined the axial liquid dispersion coefficient in a 7.8-cm bubble column with a height of 1.8 m under pressures of 3.0–7.1 atm. The superficial gas velocity varied up to 0.6 m/s. They used heat as a tracer to measure the thermal dispersion coefficient, which is comparable to the mass dispersion coefficient. They found that the effect of pressure on thermal dispersion coefficients was negligible in the pressure range of their study. Wilkinson et al. (1993) measured the liquid axial dispersion coefficient in a batch-type bubble column of 15.8 cm in diameter and 1.5 m in height for the water-nitrogen system at pressures between

Correspondence concerning this article should be addressed to L. S. Fan.

0.1 and 1.5 MPa using the electrical conductivity method. It was found that the axial liquid dispersion coefficient actually increases with increasing pressure, especially under high gas velocity conditions ($U_g > 0.10$ m/s). They noted that the available theories in the literature to describe liquid mixing under the atmospheric pressure cannot explain the pressure effect observed in their study. Their study was also limited by the narrow experimental conditions (low-pressure range and batch operation) and limited system (air-water), and the observed pressure effect needs to be further verified under a wide range of operating pressures and in different gas-liquid systems.

The most common approach to account for the nonideality of a liquid flow pattern in bubble columns is based on a one-dimensional (1-D) axial dispersion model (ADM). Because of its simplicity and ease of use, the ADM remains popular in reactor design, and numerous correlations for the axial liquid dispersion coefficient in bubble columns have been developed over the years. Most of the existing correlations were developed for air-water systems at atmospheric conditions. As a result, these correlations severely underpredict the axial dispersion coefficient in industrial reactors operating under high-pressure conditions, and cannot be applied directly to the reactor design. Tarmy et al. (1984) investigated liquid backmixing in industrial coal liquefaction reactors using radioactive tracers. The operating pressure in their study varied up to 17 MPa and they found that the measured dispersion coefficients at high pressures were up to 2.5 times smaller than the values predicted by literature correlations, which were developed based on experimental data under ambient conditions. Recently, Onozaki et al. (2000a,b) studied gas-liquid dispersion behavior in coal liquefaction reactors using a neutron absorption tracer technique. They also found that the axial dispersion coefficients of the liquid phase under coal liquefaction conditions ($P = 16.8$–18.8 MPa) were much smaller than those estimated from literature correlations obtained at ambient conditions. Those observations imply a decreasing trend for the pressure effect on liquid mixing.

In summary, although some research work has been done to study the pressure effect on liquid mixing in bubble columns, most of those studies were confined to low gas velocities or low pressures (normally less than 1.5 MPa), small column sizes, and limited systems (air-water). To date, no systematic study is available to provide comprehensive data for axial liquid dispersion coefficients at high pressures. In this study, a thermal dispersion technique is developed to measure axial liquid dispersion coefficients in bubble columns. The study is conducted in systems close to industrial applications and covers a wide range of operating conditions. The inherent mechanisms underlying the pressure effect on liquid-phase mixing are also discussed.

Experimental Studies

Measurement technique

The mixing properties of bubble columns are usually described by a 1-D dispersion model, and the dispersion coefficient can be determined by steady and unsteady tracer injection methods. It has been verified that both methods lead to the same results (Deckwer et al., 1974). For the steady injection method, a tracer is injected at the exit or at another convenient point, and the axial concentration profile is measured upward of the liquid bulk flow. The dispersion coefficient is then calculated from the axial concentration profile. With the unsteady injection method, a variable flow of tracer is injected, usually at the contactor inlet, and samples are taken at the exit. Analysis of the response curve of the tracer input yields the dispersion coefficient. Electrolyte, dye, and heat are normally applied as tracer for both methods and each of them yields identical dispersion coefficients.

In this study, the axial dispersion coefficients of the liquid phase are measured by the steady-state thermal dispersion method, that is, introducing heat close to the outlet of the liquid phase and measuring the upstream temperature profile in the liquid. The dispersion coefficient is determined from the axial temperature profile using the 1-D dispersion model. The thermal dispersion technique is based on the analogy between the mass dispersion and the heat dispersion under nonreactive conditions. Considering the energy balance for the liquid phase, the following differential equation applies

$$\frac{k_l}{\rho_l C_{pl}} \frac{d^2T}{dz^2} + \frac{U_l}{1-\epsilon_g} \frac{dT}{dz} - \frac{q}{\rho_l C_{pl}} = 0 \tag{1}$$

where q is the heat loss from the liquid phase to the surrounding environment, including the heat loss through the gas-liquid interface, through the column wall and due to liquid evaporation. In the experiments of this study, the column was insulated and the operating temperature was room temperature; therefore, the heat loss through the column wall and due to liquid evaporation would be negligibly small. The heat loss through the gas-liquid interface, which depends on the heat-transfer coefficient and temperature difference between the liquid and gas phases, would be small due to either low heat-transfer coefficient or small temperature difference. This point could be further verified as given below.

Equation 1 is comparable to the mass balance equation for the mass tracer in the liquid phase, as shown by Eq. 2 (Wendt et al., 1984)

$$D_m \frac{d^2C}{dz^2} + \frac{U_l}{1-\epsilon_g} \frac{dC}{dz} = 0 \tag{2}$$

Thus, the term in Eq. 1 corresponding to the mass dispersion coefficient can be defined as the effective thermal dispersion coefficient, that is, $E_l \equiv k_l/\rho_l C_{pl}$. The defined thermal dispersion coefficient is equivalent to the mass dispersion coefficient based on the transport analogy.

The implementation of the thermal dispersion technique can be conveniently carried out when the heat loss through the gas-liquid interface is neglected, that is, $q \approx 0$ in Eq. 1. Then, the general energy balance equation for the liquid phase, Eq. 1, is simplified to

$$\frac{k_l}{\rho_l C_{pl}} \frac{d^2T}{dz^2} + \frac{U_l}{1-\epsilon_g} \frac{dT}{dz} = 0 \tag{3}$$

In Eq. 3, z is the axial distance from the liquid outlet, and $z = 0$ represents the liquid outlet. Equation 3 can be solved

analytically after introducing the boundary conditions for a semi-infinite system, that is

$$T = T_m \quad \text{at } z = 0$$
$$T = T_0 \quad \text{at } z = \infty \tag{4}$$

where T_0 and T_m are the inlet and outlet liquid temperatures, respectively. T is the liquid temperature at a distance z from the liquid outlet. The analytical solution of Eq. 3 with the above boundary conditions is

$$\ln\left(\frac{T - T_0}{T_m - T_0}\right) = -\frac{U_l}{E_l(1-\epsilon_g)}z \tag{5}$$

Equation 5 indicates that the relationship between $\ln[(T - T_0)/(T_m - T_0)]$ and z is linear, and the thermal dispersion coefficient E_l can be calculated from the slope of the temperature profile, with the values of the gas holdup and superficial liquid velocity given. Thus, examining the linearity relationship between $\ln[(T - T_0)/(T_m - T_0)]$ and z ensures that the heat loss through gas-liquid interface is negligibly small.

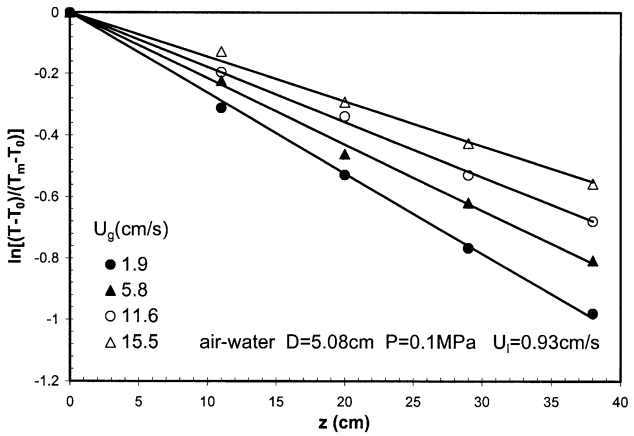

(a) water, different gas velocities

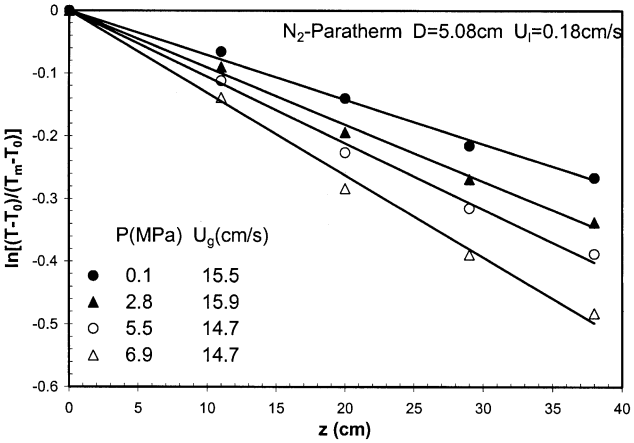

(b) Paratherm NF heat transfer fluid, different pressures

Figure 1. Temperature profiles at different gas velocity and pressure conditions.

In this study, the axial profiles of the temperature represented by $\ln[(T - T_0)/(T_m - T_0)]$ in both water and Paratherm NF heat transfer fluid measured at different gas velocity and pressure conditions are exemplified in Figure 1. The profiles shown in the figure exhibit linearity signifying indeed negligible heat loss from the liquid phase under the conditions of the present study. The validity of the thermal dispersion technique was also verified by other studies (Aoyama et al., 1968; Holcombe et al., 1983; Wendt et al., 1984).

Experimental setup

Liquid mixing experiments are conducted in two stainless steel high-pressure columns with an inner diameter of 5.08 cm and 10.16 cm, respectively. The aspect ratio for the 5.08-cm and 10.16-cm columns is 11 and 9, respectively. Three pairs of quartz windows are installed on the front and rear sides of the column, through which the bubble characteristics and flow phenomena under high-pressure conditions can be directly observed. The windows have a viewing area of 12.7 mm $\times$ 92 mm. The system pressure is controlled by a back-pressure regulator installed at the outlet of the column. Both columns can be operated up to 22 MPa. The details of the high-pressure columns were given in Luo et al. (1997). The experimental setup is shown in Figure 2.

A heater with adjustable heating power is installed in the center of the column right below the liquid outlet. The maximum heating power is 750 W. The axial temperature profile within the column is measured by several T-type copper-constantan thermocouples placed in the column center at different longitudinal positions after a steady temperature distribution is attained. The inlet temperatures of liquid and gas are kept constant during each run. Since the current high-pres-

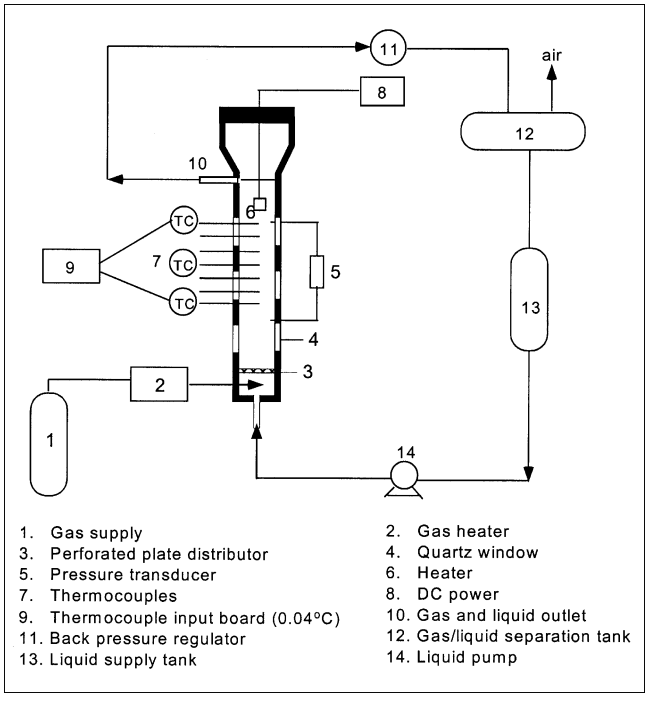

Figure 2. Experimental setup for the measurement of liquid-phase mixing.

sure system has no cooling components, in order to maintain constant liquid inlet temperature, the liquid level in the liquid supply tank is kept relatively high, and, in the meantime, the maximum temperature difference across the column is controlled to within several degrees centigrade by adjusting the heater power. Therefore, such a small amount of heat does not increase the temperature in the liquid supply tank significantly. Typically, for each run the variation of the liquid inlet temperature is less than 1°C. The compressed gas is heated to the same temperature as the inlet liquid by a gas heater. In order to prevent heat loss through the column wall, insulation materials are installed to cover the entire vessel.

The axial temperature distribution is measured by a 16-channel, high-accuracy thermocouple input board. The resolution of the board is 0.04°C for T-type thermocouples. For each gas velocity condition, 100 data points are sampled within 100 s and the average temperature is calculated. A differential pressure transducer is also installed to measure the overall gas holdup in the column simultaneously with the temperature measurement, which is required for calculating the axial dispersion coefficient. For most experiments, a perforated plate with a number of square-pitched holes of 1.6 mm in diameter and 8 mm in pitch is used as the distributor for both the gas and liquid phases. The number of holes on the plate is 45 and 120 for the 5.08-cm and 10-16 cm columns, respectively. In order to investigate the effect of distributor design on liquid mixing, two other types of distributors, porous plate and sparger, are also employed for the measurements in the 5.08-cm column. The pore size of the porous plate is 200 μm and the sparger is a 1.27-cm diameter pipe with 13 holes on the side of the pipe. The hole diameter of the sparger is 0.32 cm.

Nitrogen is used as the gas phase, and water and Paratherm NF heat-transfer fluid are used as the liquid phase. The physical properties of Paratherm NF heat-transfer fluid ($\rho_1 = 870$ kg/m^3, $\mu_1 = 0.028$ Pa·s, $\sigma = 0.029$ N/m at 27°C and 0.1 MPa) at different pressures and temperatures were given in Lin et al. (1998). The liquid is in continuous operation and the superficial liquid velocity varies up to 1.0 cm/s. The superficial gas velocity varies up to 40 cm/s which covers both the homogenous bubbling and churn-turbulent flow regimes.

Results and Discussion

Comparison with literature data

To further verify the validity of the measurement technique, liquid mixing experiments are first conducted in the air-water system under ambient conditions, and the measured axial dispersion coefficients are compared with the literature data. The effects of gas and liquid velocities on the gas holdup and the axial dispersion coefficient in the air-water system under ambient conditions are shown in Figure 3. It can be seen that the liquid velocity has an insignificant effect on the gas holdup, and the measured gas holdup values agree well with the reported literature data. It is noted that the liquid velocity is of an order of magnitude lower than the bubble rise velocity, and a significant effect of the liquid velocity on the gas holdup is not expected. The axial dispersion coefficient of the liquid phase increases significantly with increasing gas velocity. Generally, the axial liquid mixing in the nearly uniform dispersed bubbling regime is limited and the

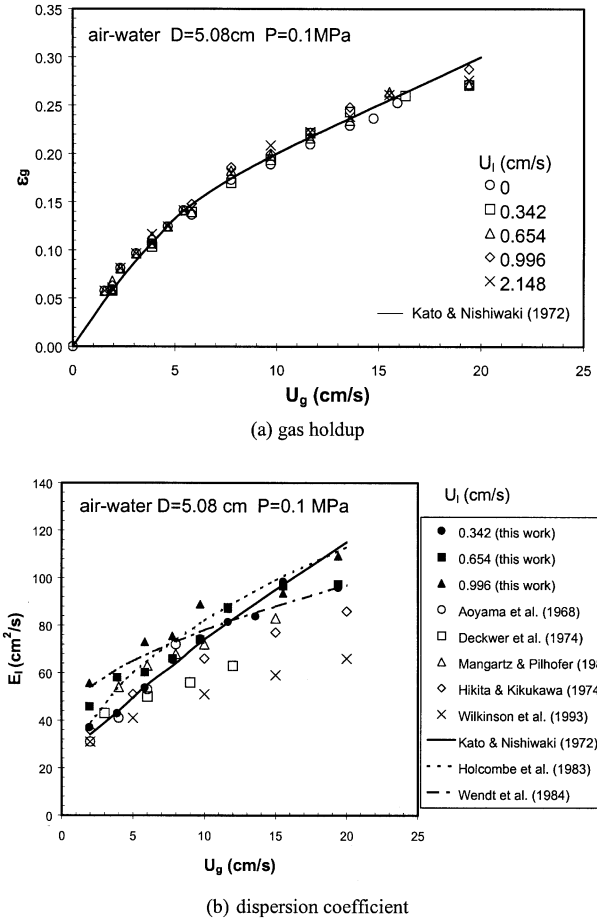

Figure 3. Experimental results vs. available literature data for the air-water system under ambient conditions.

axial dispersion coefficient is small. When the gas velocity is increased, the flow is in the coalesced bubbling or slugging regime and the nonuniform flow behavior creates significant backmixing. It is also found that the effect of liquid velocity on axial liquid mixing is small compared to the gas velocity effect. The axial dispersion coefficient in the air-water system slightly increases with an increase in the liquid velocity, especially at low gas velocities. The comparison of the measured axial dispersion coefficients with the available literature data obtained by various measurement techniques is also shown in Figure 3. Since liquid mixing strongly depends on column size, for the purpose of comparison, the literature data obtained in different sizes of columns are converted into the column size in this work (5.08 cm for Figure 3), using the relationship between the axial dispersion coefficient and the column diameter reported in literature studies. If such a relation is not available in corresponding studies, the following general relation is used to convert the data between different columns

$$E_l \propto D^{1.5} \tag{6}$$

This relation can reasonably predict the scale-up effect on liquid mixing (Deckwer et al., 1974; Wendt et al., 1984). It is

Table 1. Information Used in Figure 3 Regarding Liquid Mixing in the Air-Water System Under Ambient Conditions

Reference	Measurement Technique	U_g (cm/s)	U_l (cm/s)	D (cm)	U_l Effect	E_l vs. D
Aoyama et al. (1968)	steady injection; heat and KCl solution as tracer	0.3–8	0.18–0.62	5.0	insignificant	$E_l \propto D^{1.5}$
Kato and Nishiwaki (1972)	impulse injection; KCl solution as tracer	1–25	0.7–1.3	6.6	insignificant	N/A
Deckwer et al. (1974)	steady and impulse injection; NaCl solution as tracer	1–15	0.71	20	N/A	$E_l \propto D^{1.4}$
Hikita and Kikukawa (1974)	impulse injection; KCl solution as tracer	4.3–33.8	0	10	N/A	$E_l \propto D^{1.25}$
Mangartz and Pilhofer (1981)	steady injection; heat as tracer	0.5–18	0–6	10	insignificant	$E_l \propto D^{1.5}$
Holcombe et al. (1983)	steady injection; heat as tracer	0–60	0–2	7.8	N/A	$E_l \propto D^{1.33}$
Wendt et al. (1984)	steady injection; heat and NaCl solution as tracer	1.5–30	0.2–4.5	6.3	insignificant	$E_l \propto D^{1.4}$
Wilkinson et al. (1993)	unsteady injection; NaCl solution as tracer	2–20	0	15.8	N/A	N/A
This work	steady injection; heat as tracer	2–20	0.34–1.0	5.08	small	N/A

also noted that different gas introduction systems might be used in each study, and this difference is neglected in the data conversion. The comparison shows that the experimental data obtained in this study using the thermal dispersion technique agree well with most literature data. It is also found that the data converted from large columns (such as $D > 10$ cm) (Deckwer et al., 1974; Hikita and Kikukawa, 1974; Wilkinson et al., 1993) are lower than the experimental data actually obtained in small columns (Aoyama et al., 1968; Kato and Nishiwaki, 1972; Holcombe et al., 1983; Wendt et al., 1984). This may indicate different mixing behavior in small columns due to wall effects, and the scale-up effect on liquid mixing needs to be further investigated. Detailed information of various literature studies used in the comparison is shown in Table 1.

Effect of flow regime

In bubble columns, the dispersed gas phase moves in a continuous liquid medium, and, therefore, the behavior of the gas phase is of importance for understanding the flow characteristics. Depending on the nature of gas dispersion, two main flow regimes are normally identified in the literature: homogeneous (or dispersed) bubbling flow and churn-turbulent (or coalesced bubbling) flow. The churn-turbulent flow can be further subdivided into the vortical-spiral flow condition and the turbulent flow condition (Chen and Fan, 1992; Chen et al., 1994). In homogeneous bubbling flow regime predominating at low and intermediate gas velocities, no bubble coalescence occurs and the bubbles are of uniform, small size. In the churn-turbulent flow regime occurring at high gas velocities, bubbles coalesce intensively, and both the bubble size and rising velocity are large and exhibit wide distributions. Distinct bubble characteristics in these two flow regimes may result in different liquid mixing behaviors. Figure 4 shows the effect of flow regime on liquid mixing at different pressures. It can be seen that the axial dispersion coefficient of the liquid phase increases with increasing gas velocity, particularly in the homogeneous bubbling regime under ambient pressure. At high gas velocities, the axial dispersion coefficient tends to level off. The transition velocities from the homogeneous bubbling flow to the churn-turbulent flow indicated in Figure 4 are identified based on the drift-flux model (Luo et al., 1997). For gas-liquid flows, the drift flux of gas is defined as the volumetric flux of the gas phase relative to a surface moving at the average velocity of gas-liquid systems. This flux can be expressed using the relative velocity between the gas and liquid phases as

$$j_{gl} = \epsilon_g(1-\epsilon_g)\left(\frac{U_g}{\epsilon_g} - \frac{U_l}{\epsilon_l}\right) \tag{7}$$

Figure 5 shows the overall gas holdup and the relationship between the drift flux and the gas holdup at different pressures in the 10.16-cm column. As can be seen from Figure 5a, at low gas holdups, the drift flux increases linearly with the gas holdup, indicating the prevalence of small dispersed bubbles. When the gas holdup or gas velocity exceeds a certain

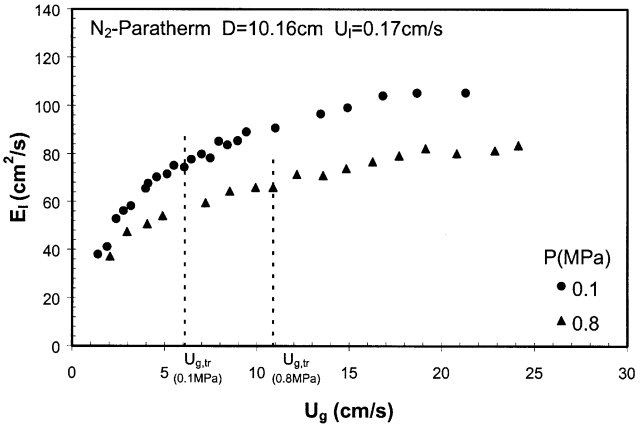

Figure 4. Gas velocity effect on the axial liquid dispersion coefficient at different pressures in the 10.16-cm column.

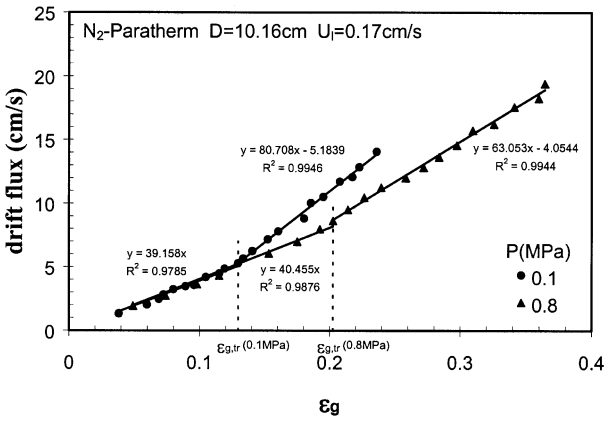

(a) drift flux vs. gas holdup

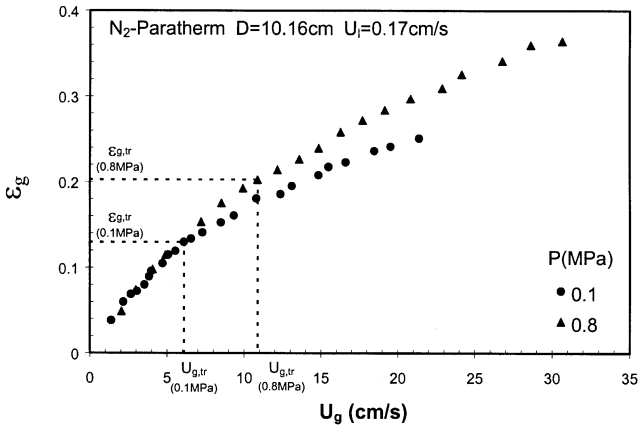

(b) gas holdup vs. gas velocity

Figure 5. Determining transition velocity from homogeneous bubbling to churn-turbulent flow regimes at different pressures.

value, the increase rate of drift flux with the gas holdup become larger, which indicates the existence of large coalesced bubbles. The point at which the increased rate of drift flux suddenly changes can be defined as the onset of the churn-turbulent flow. At both ambient and elevated pressures, the increased rates of drift flux with gas holdup are almost identical in the homogeneous bubbling regime. In contrast, in the churn-turbulent flow regime, the increased rate of drift flux at ambient pressure is higher than that at elevated pressure because the bubbles become smaller and more uniform at elevated pressure. From Figure 5b, it is found that there is no significant difference in the gas holdup when the flow under both pressures is in the homogeneous bubbling regime; however, in the churn-turbulent flow regime, the gas holdup at the elevated pressure is much higher than that at the ambient pressure due to the smaller bubble size. The transition velocities identified based on the drift-flux method for the N_2-Paratherm liquid system at ambient pressure and the pressure of 0.8 MPa are about 6.0 cm/s and 11.0 cm/s, respectively. Increasing the system pressure markedly delays the transition from the homogeneous bubbling to the churn-turbulent flow regime. In other words, the existence of small bubbles in the system tends to delay the regime transition. In order to further verify the validity of the drift-flux method, the transition point in the air-water system under ambient pressure is also identified using the same approach. It is found that the transition velocity for the air-water system under ambient conditions is about 5.0 cm/s, and agrees with most literature data which are in the range of 4.0–5.2 cm/s, as shown in Table 2. Since the bubble size in the Paratherm liquid is normally smaller than that in water due to lower surface tension, the transition velocity in the Paratherm liquid (about 6.0 cm/s) is expected to be higher than that in the water (about 5.0 cm/s).

It is generally accepted that liquid-phase turbulence induced mainly by the movement of bubbles and the existence of large-scale liquid internal circulation are the main causes of liquid mixing in bubble columns. Many studies have indicated the presence of a large-scale liquid circulation cell in bubble columns, with liquid ascending in the central region and descending in the wall region (Joshi, 1980; Degaleesan et al., 1997). Liquid internal circulation is mainly driven by nonuniform radial gas distribution in the column. In the homogeneous bubbling flow regime, there is no pronounced large-scale liquid circulation in the column and the liquid-phase turbulence induced by rising bubbles is the main reason for liquid mixing. The scale of turbulence in the homogeneous bubbling flow regime depends on the bubble size. As the gas velocity increases, the bubble size increases and, thus, the bubble-induced turbulence increases, resulting in a rapid increase in the axial dispersion coefficient, as shown in Figure 4. In the churn-turbulent flow regime, both the convective liquid circulation and the liquid turbulent fluctuations play important roles in determining the mixing behavior of the liquid phase. The scale of turbulence in this flow regime

Table 2. Literature Data Regarding Regime Transition Velocity for the Air-Water System under Ambient Conditions

Reference	Transition Vel. (cm/s)	Identification Method
Rice and Littlefield (1987)	4.0	Based on experimental gas holdup and liquid mixing data
Shnip et al. (1992)	4.4–5.2	Based on linear stability theory
Drahos et al. (1992) Zahradnik et al. (1994)	4.0	Based on experimental gas holdup and gas mixing data
Reese and Fan (1994)	4.2	Based on experimental gas holdup data measured by PIV technique
Bakshi et al. (1995)	4.8	Based on wavelet-based multiresolution analysis of local gas holdup signals
Hyndman and Guy (1995)	4.5	Based on experimental gas holdup data

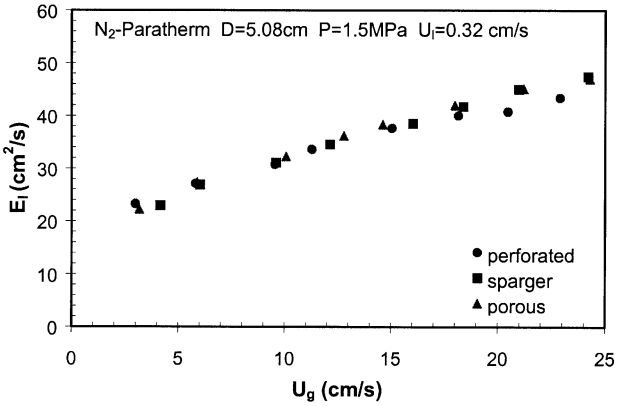

(a) dispersion coefficient

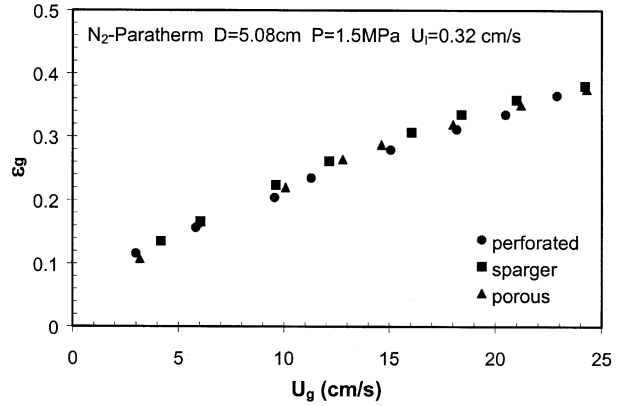

(b) gas holdup

Figure 6. Distributor design effects on liquid mixing and gas holdup in the 5.08-cm column at elevated pressure.

is proportional to the column diameter, and the intensity of the turbulence is not enhanced significantly by increasing gas velocity. Instead, increasing gas velocity induces an enhanced liquid internal circulation, which does not improve the mixing as efficiently as the local turbulent fluctuation does. Therefore, the axial dispersion coefficient levels off at high gas velocities. Similar observations were also found for heat-transfer coefficients in bubble columns (Deckwer, 1980; Yang et al., 2000).

The effect of distributor design on the hydrodynamics and liquid-phase mixing in bubble columns is also investigated in this study. Three types of distributor plates are employed, that is, perforated plate, porous plate, and sparger. Detailed information about the configuration of these distributors can be found in the experimental section. Figure 6 shows the experimental results of gas holdup and axial dispersion coefficients using different types of distributors in the 5.08-cm column at an elevated pressure. It can be seen that the effects of distributor design on both the gas holdup and axial dispersion coefficients are insignificant. It is commonly accepted that the distributor only affects a certain flow region above it,

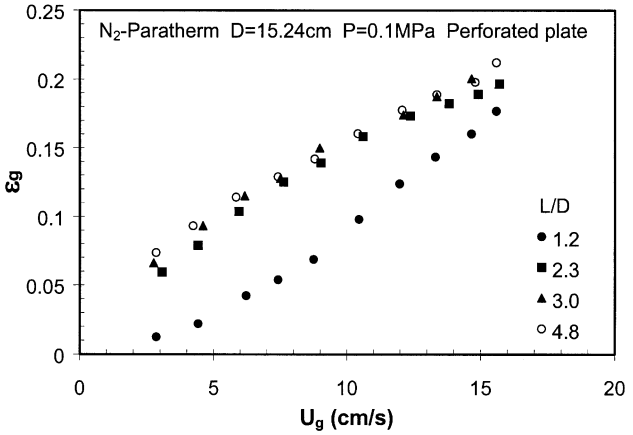

Figure 7. Gas holdups measured at different axial positions in a 15.24-cm-bubble column at ambient conditions.

that is, in the area of height to diameter ratio less than 3.0 or even lower. Reese and Fan (1994) studied the transient flow structure in the entrance region of a bubble column using the particle image velocimetry technique. They found that the length of the entrance region affected by the distributor depends on the gas velocity. When the superficial gas velocity is higher than 3.0 cm/s, which is the typical experimental condition in this work, the entrance effects become insignificant and only a short height immediately above the distributor is required for the coherent flow structure to be developed. Figure 7 shows the gas holdups measured at different axial positions in a 15.24-cm bubble column at ambient conditions. It can be seen that the variation of gas holdup with the axial position becomes insignificant when the dimensionless axial height (L/D) is higher than 2.0–3.0. Since the measurements of gas holdup and axial dispersion coefficients in this study are conducted in the well-developed flow region ($L/D > 3.0$), no significant distributor effect is expected. On the other hand, the wall effects in small columns may also help offset the gas distributor effect.

Effect of system pressure

The effect of pressure on the axial dispersion coefficient in the 5.08-cm and 10.16-cm columns for the nitrogen-Paratherm liquid system is shown in Figures 8 and 9, respectively. It is found that the axial dispersion coefficient decreases significantly when the pressure is changed from the ambient to elevated pressures in both columns, indicating distinct flow behavior under ambient and elevated pressures. When the pressure is further increased, the decrease rate of the axial dispersion coefficient becomes smaller. The pressure effect is more pronounced at high gas velocities and in large columns. For example, as shown in Figure 8a, at a gas velocity of 20 cm/s and a liquid velocity of 0.18 cm/s, when the pressure increases from 0.1 MPa to 10.3 MPa (a factor of 103 increase), the axial dispersion coefficient in the 5.08-cm column decreases from 40 cm^2/s to 18 cm^2/s, that is a 55% decrease. In contrast, under similar gas and liquid velocities, the axial dispersion coefficient in the 10.16-cm column decreases from 104 cm^2/s to 40 cm^2/s (a 62% decrease) as the pressure varies

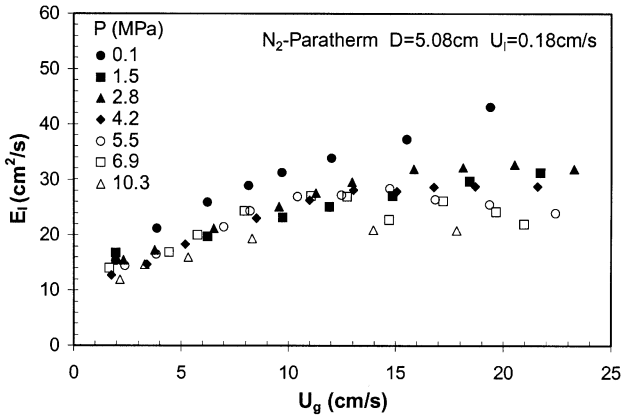

(a) U_l=0.18cm/s

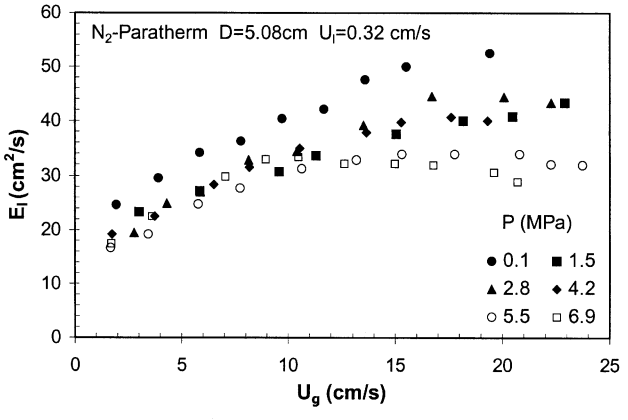

(b) U_l=0.32cm/s

Figure 8. Pressure effect on liquid-phase mixing in the 5.08-cm column at different liquid velocities.

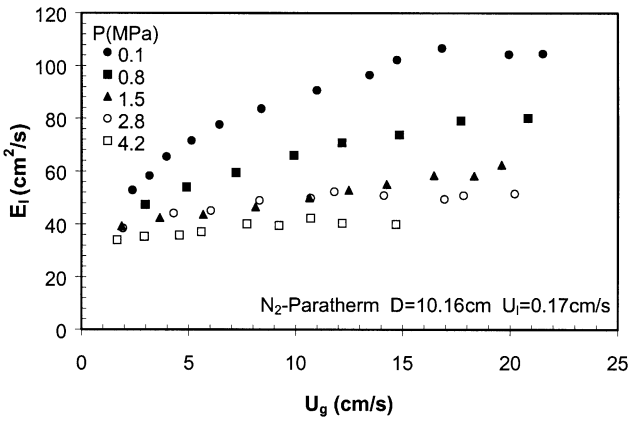

(a) U_l=0.17cm/s

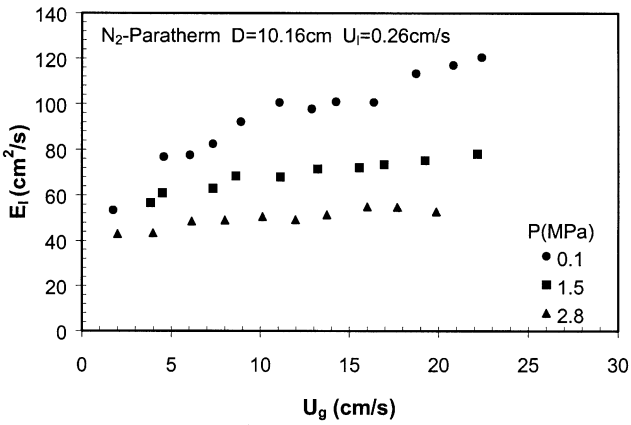

(b) U_l=0.26cm/s

Figure 9. Pressure effect on liquid-phase mixing in the 10.16-cm column at different liquid velocities.

only from 0.1 MPa to 4.2 MPa (a factor of 42 increase), as shown in Figure 9a. Reduced liquid backmixing at high pressures was also observed by other researchers (Tarmy et al., 1984; Onozaki et al., 2000a,b). The insignificant pressure effect on liquid mixing in small columns (diameter normally less than 10.0 cm) observed by some researchers (Holcombe et al., 1983; Houzelot et al., 1985) is possibly due to the narrow operating conditions in their studies, that is, either low gas velocities or a narrow pressure range. As shown in Figure 8, in small columns, the variation of axial dispersion coefficients with pressure is not pronounced at low gas velocities (that is, in the homogeneous bubbling flow regime).

The gas holdup in both the 5.08-cm and 10.16-cm columns for the nitrogen-Paratherm liquid system at different pressures are shown in Figure 10. As shown in the figure, the gas holdup increases significantly with increasing pressure, particularly in the low-pressure range ($P < 4.2$ MPa). When the pressure is further increased, the gas holdup slightly increases with pressure. A higher gas holdup at elevated pressures indicates the existence of small bubbles in the system.

The available theories in the literature describing liquid mixing under atmospheric pressure are based on either liquid turbulence induced by rising bubbles (Baird and Rice, 1975), large-scale liquid internal circulation (Joshi, 1980), or a combination of these two mechanisms (Degaleesan et al., 1997). Based on the internal circulation model, Joshi (1980) proposed the following equation to predict the average liquid circulation velocity in bubble columns

$$V_c = 1.31\left[gD\left(U_g - \frac{\epsilon_g}{1-\epsilon_g}U_l - \epsilon_g U_{b\infty}\right)\right]^{1/3} \qquad (8)$$

where $U_{b\infty}$ is the terminal bubble rise velocity. The second term on the righthand side of Eq. 8 is normally negligible compared to the other two terms at low liquid velocities. It can be seen that both the gas holdup and bubble rise velocity affect the liquid circulation velocity, which can be treated as a measure of the extent of liquid circulation effect on liquid mixing. It is known that the gas holdup increases and the bubble size and rise velocity decrease with increasing pressure. Based on Eq. 8, the combined effects of gas holdup and bubble rise velocity on the liquid circulation velocity may re-

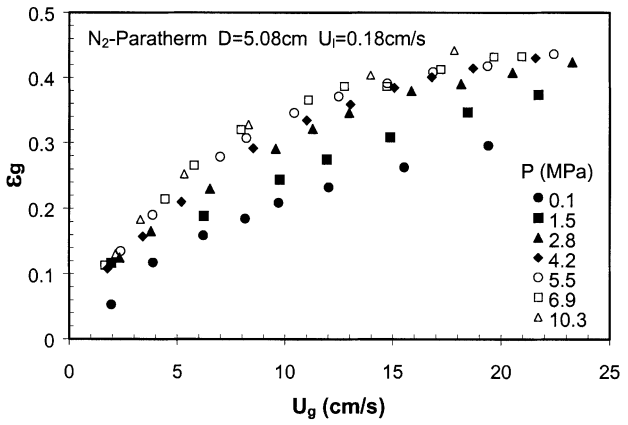

(a) 5.08-cm column

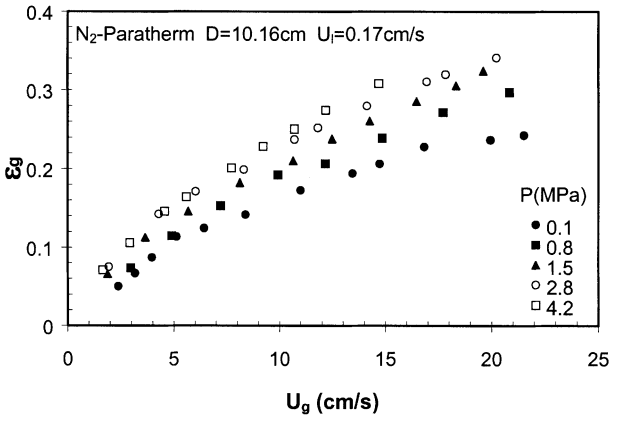

(b) 10.16-cm column

Figure 10. Pressure effect on the gas holdup in both the 5.08-cm and 10.16-cm columns.

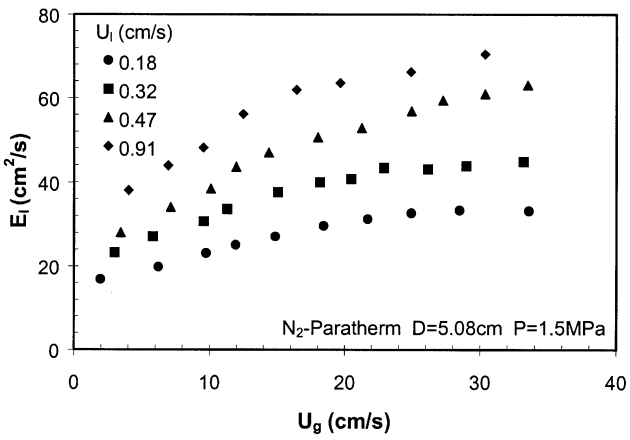

(a) 5.08-cm column

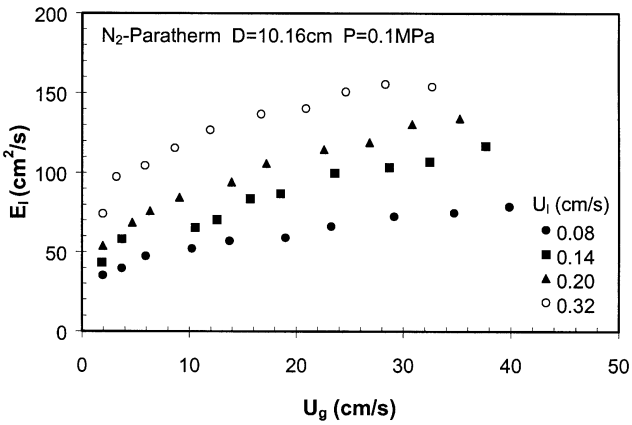

(b) 10.16-cm column

Figure 11. Effect of liquid-phase motion on liquid mixing in both the 5.08-cm and 10.16-cm columns.

sult in unchanged or slightly changed liquid circulation pattern at elevated pressures. On the other hand, when the system pressure increases, bubbles become smaller, and liquid entrainment by bubble wakes and turbulence induced by the motion of bubbles are reduced. Therefore, the extent of liquid mixing is reduced at elevated pressures. Our recent study of flow fields and Reynolds stresses in high-pressure bubble columns using the laser Doppler velocimetry technique (Lee et al., 2001) also confirmed that the bubble-induced turbulence of the liquid phase is depressed as the pressure increases. The combined variations of liquid-phase turbulent fluctuations and internal liquid circulation give rise to the overall effect of pressure on liquid mixing.

Effect of liquid velocity

The effects of liquid velocity on liquid mixing and gas holdup in both columns are shown in Figures 11 and 12, respectively. It is sound that the effect of liquid velocity on the gas holdup is insignificant, indicating that the liquid-phase motion has little effect on bubble characteristics under low liquid velocity conditions (superficial liquid velocity less than 1.0 cm/s in this study). On the other hand, liquid-phase mixing is enhanced significantly with increasing liquid velocity in the range of this study. Comparing Figure 11 to Figure 3, it is found that the effect of liquid velocity on liquid mixing in the nitrogen-Paratherm liquid system is more pronounced than that in the air-water system. It is also noted that under the same liquid velocity, the Reynolds number for water is about 33 times higher than that for the Paratherm liquid used in this study. Although many studies reported in the literature indicate a weak relation between the axial dispersion coefficient and the liquid velocity for water or aqueous liquids, there are some studies that indicate a strong relation; no study is available for highly viscous liquids such as Paratherm heat-transfer fluid used in this study. Zahradnik et al. (1997) studied axial liquid mixing in a bubble column using different liquids, and found that the axial dispersion coefficient increases with increasing liquid flow rate within the entire liquid velocity range of their study (superficial liquid velocity from 0.4 cm/s to 1.1 cm/s); the type of the liquid medium used for obtaining this set of data was not specified in their article.

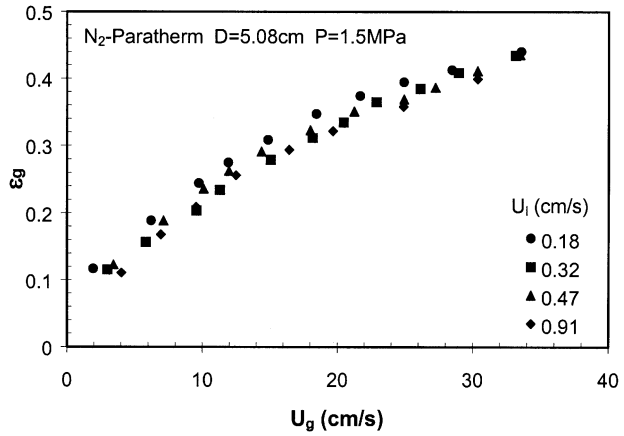

(a) 5.08-cm column

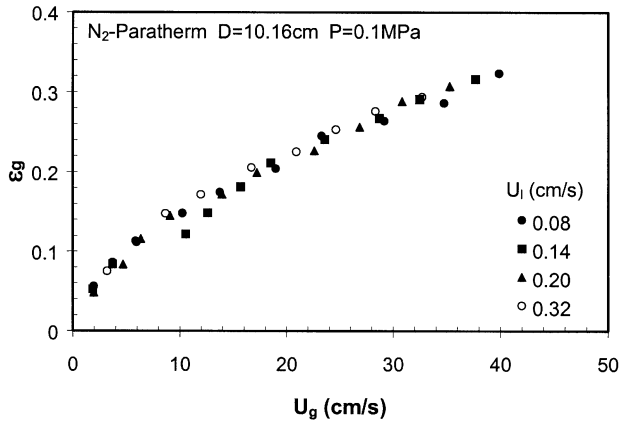

(b) 10.16-cm column

Figure 12. Effect of liquid velocity on the gas holdup in both the 5.08-cm and 10.16-cm columns.

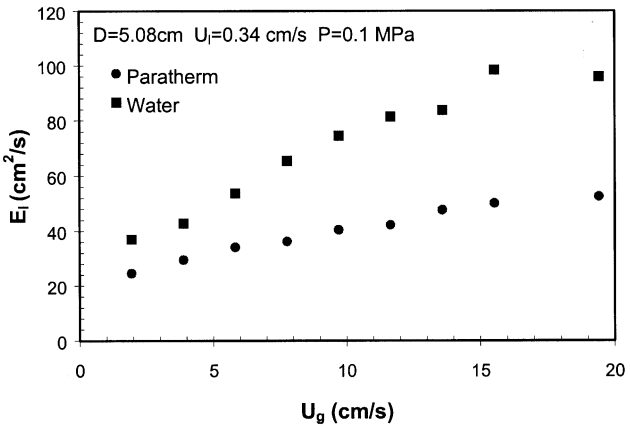

(a) dispersion coefficient

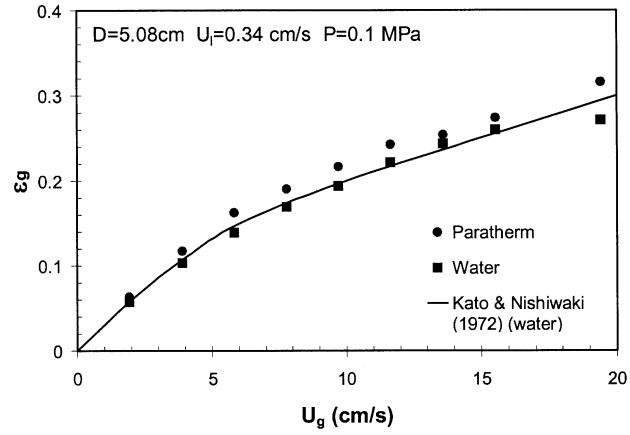

(b) gas holdup

Figure 13. Axial dispersion coefficient and gas holdup in water vs. in Paratherm NF heat-transfer fluid at ambient pressure.

The enhancement of liquid-phase mixing with increasing liquid velocity is probably due to the enhanced liquid-phase turbulence. Turbulent fluctuations in the liquid phase are important in determining the mixing behavior, and are mainly caused by two factors: the movement of bubbles and turbulent liquid eddies. Under low liquid velocity conditions, liquid-phase motion does not change bubble characteristics significantly and, hence, does not affect bubble-induced turbulence; however, liquid-phase motion does enhance the energy exchange between microscale liquid eddies. Therefore, it enhances the overall turbulent fluctuations in the liquid phase yielding higher dispersion coefficients observed at higher liquid velocities. When the system pressure increases, the bubble-induced turbulence is depressed due to smaller bubble size and reduced bubble velocity, and liquid eddy induced turbulence may play a more prominent role in determining liquid mixing. Further study on turbulence mechanisms in two-phase flow systems is needed for better understanding of liquid backmixing.

In this study, the axial dispersion coefficients in the air-water system are also measured at the ambient pressure. Figure 13 shows the comparison of liquid mixing and gas holdup between water and Paratherm NF heat-transfer fluid at ambient pressure. As shown in Figure 13, the gas holdup in Paratherm liquid is higher than that in water, indicating a smaller bubble size in the Paratherm liquid. The measured gas holdup data in the air-water system also agree with the literature data obtained in the column of similar size (Kato and Nishiwaki, 1972). Paratherm liquid has a higher viscosity and a lower surface tension compared to water. Higher liquid viscosity results in larger bubble size and, thus, lower gas holdup (Zahradnik et al., 1997), while lower surface tension favors the formation of small bubbles and, thus, increases gas holdup. The combination of these two effects gives rise to the overall gas holdup in the Paratherm liquid. According to the comparison of gas holdup between the water and Paratherm liquid as shown in Figure 13, the effect of surface tension on bubble size and gas holdup is more pronounced compared to the viscosity effect, resulting in smaller bubble size and higher gas holdup in the Paratherm liquid.

A comparison of liquid mixing between these two liquids shows higher axial dispersion coefficients in the Paratherm

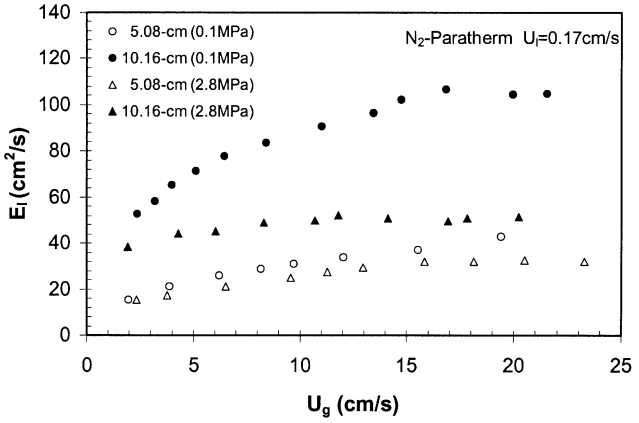

(a) dispersion coefficient

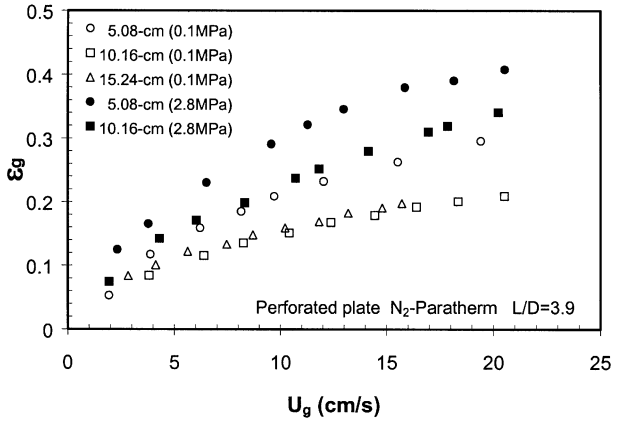

(b) gas holdup

Figure 14. Axial liquid dispersion coefficient and gas holdup in the 5.08-cm column vs. in the 10.16-cm column at different pressures.

liquid at the same gas and liquid velocities. The difference becomes more pronounced with increasing gas velocity. Bubbles in water are generally larger than those in Paratherm liquid, resulting in enhanced bubble-induced turbulence. Therefore, the axial dispersion coefficients are higher for water than those for Paratherm liquid. Based on this comparison, it is clear that axial dispersion coefficients obtained in water cannot be used directly to design bubble column reactors when a nonaqueous liquid medium is used.

Effect of column size

Mixing behavior strongly depends on column size and it is necessary to study the scale-up effect of liquid-phase mixing. In this study, the mixing experiments are carried out in both the 5.08-cm and 10.16-cm columns. The effects of column size on the gas holdup and axial dispersion coefficient can be seen clearly from Figure 14. The gas holdup in the 5.08-cm column is much higher than that in the 10.16-cm column at both ambient and elevated pressures. This difference is more pronounced in the churn-turbulent flow regime. For example, at ambient pressure and a gas velocity of 20 cm/s, the gas holdup in the 5.08-cm and 10.16-cm columns is 0.21 and 0.30, respectively (about a 43% difference). When the pressure increases, the difference in the gas holdup between these two columns tend to be reduced. In order to further confirm the effect of column size, the gas holdup at ambient conditions is also measured in a larger column (15.24 cm in diameter) at the same dimensionless axial position ($L/D = 3.9$) using the same liquid and the same type of distributor plate. The gas holdup data in the 15.24-cm column are also shown in Figure 14b. It can be seen that the difference between gas holdups in the 10.16-cm and 15.24-cm columns is small, which indicates that the effect of the column size on the gas holdup becomes smaller with increasing column diameter. Figure 15 further shows the effect of column size on the gas holdup at ambient conditions in the air-water system obtained in this study and those reported in the literature. In the figure, the column diameter is up to 5.5 m. The solid line in the figure represents the predictions by the gas holdup correlation developed by Luo et al. (1999), which was mainly based on experimental data in columns of diameter larger than 10 cm. As shown in the figure, when the column diameter increases, the difference in gas holdup becomes smaller. Shah et al. (1982) and Reilly et al. (1986) also found that the effect of column size on the gas holdup is small when the column diameter increases to a certain size (0.1 to 0.15 m in their study).

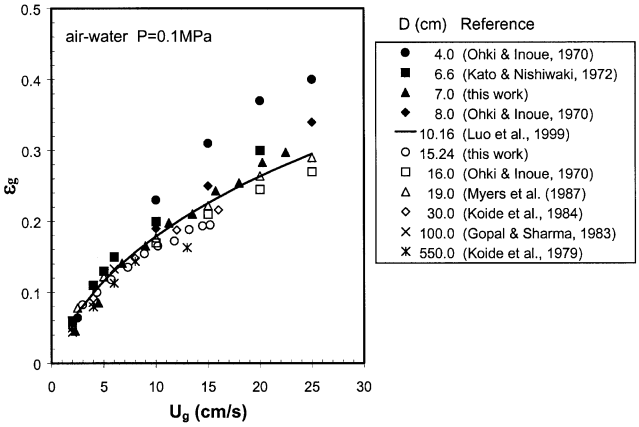

Figure 15. Gas holdup data obtained in different sizes of columns under ambient conditions for the air-water system.

The effect of the column size on gas holdup occurs mainly through the variation in bubble characteristics. In small columns, the column wall effect is significant and the bubble size is confined by the column size, particularly in the slugging and churn-turbulent flow regimes. Therefore, the gas holdup in small columns is higher. When the column is larger than a certain size, the wall effect is negligible and, thus, the bubble size no longer depends on the column dimension. In this situation, the bubble size is mainly determined by the rates of bubble coalescence and breakup, and, therefore, the gas holdup is no longer affected by the column size.

The effect of column size on the axial liquid dispersion coefficient is shown in Figure 14a. It is found that the axial dispersion coefficient strongly depends on the column size

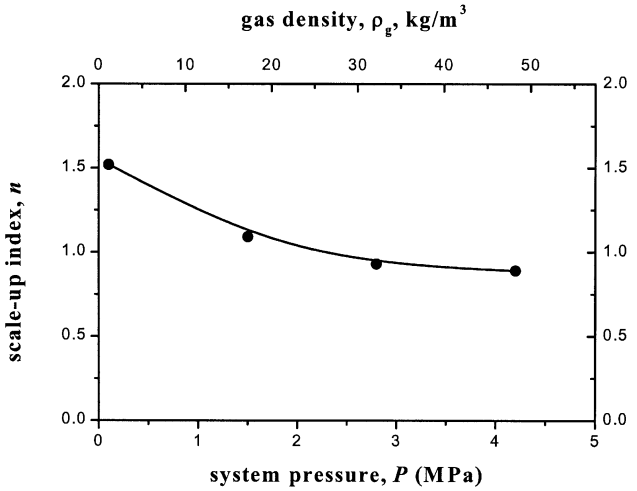

Figure 16. Pressure effect on the scale-up index of liquid-phase mixing.

and liquid backmixing in the larger column is more apparent. As mentioned earlier, liquid-phase mixing is mainly determined by liquid-phase turbulence and large-scale liquid internal circulation. Both the scale of turbulence and the extent of liquid circulation strongly depend on the column size. Liquid turbulence and internal circulation are stronger in larger columns. Therefore, liquid mixing is enhanced significantly with increasing column size. The relationship between the axial dispersion coefficient and the column diameter is commonly expressed by

$$E_l \propto D^n \tag{9}$$

Many studies have shown that the scale-up index n is in the range of 1.4–1.5 at ambient conditions (Deckwer et al., 1974; Wendt et al., 1984). As shown in Figure 14a, the effect of column size on liquid mixing is reduced with increasing pressure. Based on the experimental data in this study, the values of the scale-up index at different pressures are shown in Figure 16. As can be seen, at ambient pressure, the index is about 1.5, which agrees with most literature studies. When the pressure increases, the index decreases significantly. At high pressures, the values of the index are in the range of 0.9–1.0. The variation of scale-up index with gas density can be expressed by the following relation

$$1 - \frac{n}{n_0} = 0.11 \ln\left(\frac{\rho_g}{\rho_{g0}}\right) \tag{10}$$

Here, n_0 ($= 1.5$) is the value of the scale-up index at ambient pressure, and ρ_{g0} is the density of gas at ambient pressure.

The reduced effect of column size on the liquid mixing behavior at high pressures is mainly due to the variation of bubble characteristics. At ambient pressure, bubbles are large and unstable, and the behavior of large bubbles is easily affected by the column wall, while at elevated pressures, the bubble size is reduced significantly and small bubbles tend to be more stable. The effect of column size on the behavior of small bubbles is not as significant as that on the behavior of large bubbles. Therefore, the effect of column size on liquid mixing is reduced at elevated pressures.

Table 3. Axial Dispersion Coefficients: Measured in an Industrial Reactor vs. Calculated Based on the Scale-Up Relation

Parameters	Onozaki et al. (2000a)	This Work
Column diameter, m	1.0	0.102
Gas source	Mainly H_2	N_2
Operating pressure, MPa	16.6–16.8	1.8
Operating temperature, °C	40	27
Gas density inside reactor, kg/m^3	20	20
Liquid density, kg/m^3	964	872
Liquid viscosity, mPa·s	7.0	28
Superficial gas velocity, cm/s	6.3	6.2
Superficial liquid velocity, cm/s	0.31	0.32
Axial dispersion coeff., cm^2/s	1,100 (measured) 670 (simulated)	67
Axial dispersion coeff., cm^2/s*	1,100 (measured) 670 (simulated)	688

*Converting the condition of this work to that of Onozaki et al. (2000a) using the scale-up index (n) of 1.02 (Figure 16) for ρ_g of 20 kg/m^3.

Based on the scale-up relation (Eq. 9), the axial dispersion coefficient in industrial reactors can be estimated from the data in smaller laboratory-scale columns. Table 3 shows an example of a comparison between the axial dispersion coefficient actually measured in an industrial reactor and that calculated from the data in a laboratory-scale column based on the scale-up relation. The measured and simulated axial dispersion coefficients in the industrial reactor (1 m in diameter) are 1,100 and 670 cm^2/s, respectively, under the conditions listed in Table 3 (Onozaki et al., 2000a). The axial dispersion coefficient measured in the 10.16-cm column of this study under a condition of matched gas density and superficial gas and liquid velocities of 67 cm^2/s. Considering the scale-up index (n) of 1.02 for the gas density of 20 kg/m^3, the axial dispersion coefficient for the 1-m column can be estimated to be 688 cm^2/s based on the present result for the 10.16-cm column, which is comparable to the reported measured (1,100 cm^2/s) or simulated (670 cm^2/s) value. If, however, the scale-up index value of 1.5 for the ambient pressure is used, the estimated axial dispersion coefficient for the 1-m column becomes 2,057 cm^2/s, which would be much higher than the reported measured or simulated value. This example illustrates the importance of considering the variation of liquid mixing characteristics with pressure in the scale-up process.

Concluding Remarks

The thermal dispersion technique is developed to determine axial dispersion coefficients of the liquid phase at high pressure in the system close to industrial applications. The validity of the measuring technique is verified by the comparison of the measured results with the literature data. The study covers a wide range of operating gas velocity and pressure conditions. The axial liquid dispersion coefficient is found to increase with increasing gas velocity and decrease with increasing pressure. Liquid properties, liquid-phase motion, and column dimension have significant effects on liquid-phase mixing; however, distributor design does not have

a significant effect. Liquid mixing in bubble columns is controlled by the combined mechanism of local liquid turbulence and large-scale liquid internal circulation. Local turbulent fluctuation of the liquid phase is caused by the movement of both bubbles and turbulent liquid eddies.

Acknowledgment

This work was supported by the National Science Foundation Grant CTS-9906591 and the U.S. Department of Energy Grant DEFC22-95 PC 95051 with Cooperative Agreement with Air Products and Chemicals, Inc. The helpful assistance of Mr. Vivek Lal on the measurement of gas holdups in the 15.24-cm column is gratefully acknowledged.

Notation

C = concentration of mass tracer, mol/m^3
C_{pl} = heat capacity of liquid, J/(kg·°C)
D = column diameter, m
D_m = mass dispersion coefficient, m^2/s
E_l = thermal dispersion coefficient, m^2/s
g = gravitational acceleration, m/s^2
j_{gl} = drift flux of gas, m/s
k_l = thermal conductivity of liquid, W/(m·°C)
L = axial height above distributor, m
n = scale-up index for liquid mixing, dimensionless
n_0 = scale-up index for liquid mixing at ambient pressure, dimensionless
P = system pressure, Pa
q = heat loss from the liquid phase to the surrounding environment, W/m^3
T = temperature at axial position z, °C
T_0 = liquid inlet termperature, °C
T_m = liquid outlet temperature, °C
$U_{b\infty}$ = terminal bubble rising velocity, m/s
U_g = superficial gas velocity, m/s
$U_{g,tr}$ = regime transition velocity, m/s
U_l = superficial liquid velocity, m/s
V_c = average liquid circulation velocity, m/s
z = axial distance from the liquid outlet, m

Greek letters

ϵ_g = gas holdup, dimensionless
$\epsilon_{g,tr}$ = gas holdup at the regime transition point, dimensionless
ϵ_l = liquid holdup, dimensionless
μ_l = liquid viscosity, Pa·s
ρ_g = gas density, kg/m^3
ρ_{g0} = gas density at ambient pressure, kg/m^3
ρ_l = liquid density, kg/m^3
σ = surface tension, N/m

Literature Cited

Aoyama, Y., K. Ogushi, K. Koide, and H. Jubota, "Liquid Mixing in Concurrent Bubble Columns," *J. Chem. Eng. Japan*, **1**, 158 (1968).
Baird, M., and R. Rice, "Axial Dispersion in Large Scale Unbaffled Columns," *Chem. Eng. J.*, **9**, 171 (1975).
Bakshi, B. R., H. Zhong, P. Jiang, and L. S. Fan, "Analysis of Flow in Gas-Liquid Bubble Columns Using Multi-Resolution Methods," *Chem. Eng. Res. Des.*, **73**, 608 (1995).
Chen, R. C., and L. S. Fan, "Particle Image Velocimetry for Characterizing the Flow Structure in Three-Dimensional Gas-Liquid-Solid Fluidized Beds," *Chem. Eng. Sci.*, **47**, 3615 (1992).
Chen, R. C., J. Reese, and L. S. Fan, "Flow Structure in a Three-Dimensional Bubble Column and Three-Phase Fluidized Bed," *AIChE J.*, **40**, 1093 (1994).
Deckwer, W. D., "On the Mechanism of Heat Transfer in Bubble Column Reactors," *Chem. Eng. Sci.*, **35**, 1341 (1980).
Deckwer, W. D., R. Burckhart, and G. Zoll, "Mixing and Mass Transfer in Tall Bubble Columns," *Chem. Eng. Sci.*, **29**, 2177 (1974).
Degaleesan, S., M. P. Dudukovic, B. A. Toseland, and B. L. Bhatt, "A Two-Compartment Convective-Diffusion Model for Slurry Bubble Column Reactors," *Ind. Eng. Chem. Res.*, **36**, 4670 (1997).
Drahos, J., J. Zahradnik, M. Fialova, and F. Bradka, "Identification and Modeling of Liquid Flow Structures in Bubble Column Reactors," *Chem. Eng. Sci.*, **47**, 3313 (1992).
Gopal, J. S., and M. M. Sharma, "Mass Transfer Characteristics of Low H/D Bubble Columns," *Can. J. Chem. Eng.*, **61**, 517 (1983).
Hikita, H., and H. Kikukawa, "Liquid-Phase Mixing in Bubble Columns: Effect of Liquid Properties," *Chem. Eng. J.*, **8**, 191 (1974).
Holcombe, N. T., D. S. Smith, H. N. Knickle, and W. O'Dowd, "Thermal Dispersion and Heat Transfer in Nonisothermal Bubble Columns," *Chem. Eng. Commun.*, **21**, 135 (1983).
Houzelot, J. L., M. F. Thiebaut, J. C. Charpentier, and J. Schiber, "Contribution to the Hydrodynamic Study of Bubble Columns," *Int. Chem. Eng.*, **25**, 645 (1985).
Hyndman, C. L., and C. Guy, "Gas Phase Hydrodynamics in Bubble Columns," *Chem. Eng. Res. Des.*, **73**, 302 (1995).
Joshi, J. B., "Axial Mixing in Multiphase Contactors—a Unified Correlation," *Trans. Instn. Chem. Engrs.*, **58**, 155 (1980).
Kato, Y., and A. Nishiwaki, "Longitudinal Dispersion Coefficient of a Liquid in a Bubble Column," *Int. Chem. Eng.*, **12**, 182 (1972).
Koide, K., S. Morooka, K. Ueyama, A. Matsuura, F. Yamashita, S. Iwamoto, Y. Kato, H. Inoue, M. Shigeta, S. Suzuki, and T. Akehata, "Behavior of Bubbles in Large Scale Bubble Column," *J. Chem. Eng. Japan*, **12**, 98 (1979).
Koide, K., A. Takazawa, M. Komura, and H. Matsunaga, "Gas Holdup and Volumetric Liquid-Phase Mass Transfer Coefficient in Solid-Suspended Bubble Columns," *J. Chem. Eng. Japan*, **17**, 459 (1984).
Lee, D. J., B. K. McLain, Z. Cui, and L. S. Fan, "Pressure Effect on the Flow Fields and the Reynolds Stresses in a Bubble Column," *Ind. Eng. Chem. Res.*, **40**, 1442 (2001).
Lin, T. J., K. Tsuchiya, and L. S. Fan, "Bubble Flow Characteristics in Bubble Columns at Elevated Pressure and Temperature," *AIChE J.*, **44**, 545 (1998).
Luo, X., P. Jiang, and L. S. Fan, "High-Pressure Three-Phase Fluidization: Hydrodynamics and Heat Transfer," *AIChE J.*, **43**, 2432 (1997).
Luo, X., D. J. Lee, R. Lau, G. Q. Yang, and L. S. Fan, "Maximum Stable Bubble Size and Gas Holdup in High-Pressure Slurry Bubble Columns," *AIChE J.*, **45**, 665 (1999).
Mangartz, K. H., and T. H. Pilhofer, "Interpretation of Mass Transfer Measurements in Bubble Columns Considering Dispersion of Both Phases," *Chem. Eng. Sci.*, **36**, 1069 (1981).
Myers, K. J., M. P. Dudukovic, and P. A. Ramachandran, "Modelling Churn-Turbulent Bubble Columns—I. Liquid-Phase Mixing," *Chem. Eng. Sci.*, **42**, 2301 (1987).
Ohki, Y., and H. Inoue, "Longitudinal Mixing of the Liquid Phase in Bubble Columns," *Chem. Eng. Sci.*, **25**, 1 (1970).
Onozaki, M., Y. Namiki, N. Sakai, M. Kobayashi, Y. Nakayama, T. Yamada, and S. Morooka, "Dynamic Simulation of Gas-Liquid Dispersion Behavior in Coal Liquefaction Reactors," *Chem. Eng. Sci.*, **55**, 5099 (2000a).
Onozaki, M., Y. Namiki, H. Ishibashi, T. Takagi, M. Kobayashi, and S. Morooka, "Steady-State Thermal Behavior of Coal Liquefaction Reactors Based on NEDOL Process," *Energy & Fuels*, **14**, 355 (2000b).
Reese, J., and L. S. Fan, "Transient Flow Structure in the Entrance Region of a Bubble Column Using Particle Image Velocimetry," *Chem. Eng. Sci.*, **49**, 5623 (1994).
Reilly, I. G., D. S. Scott, T. De Bruijn, A. Jain, and J. Piskorz, "A Correlation for Gas Holdup in Turbulent Coalescing Bubble Columns," *Can. J. Chem. Eng.*, **64**, 705 (1986).
Rice, R. G., and M. N. Littlefield, "Dispersion Coefficients for Ideal Bubbly Flow in Truly Vertical Columns," *Chem. Eng. Sci.*, **42**, 2043 (1987).
Sangnimnuan, A., G. N. Prasad, and J. B. Agnew, "Gas Hold-Up and Backmixing in a Bubble-Column Reactor Under Coal-Hydroliquefaction Conditions," *Chem. Eng. Commun.*, **25**, 193 (1984).
Shah, Y. T., B. G. Kelkar, S. P. Godbole, and W. D. Deckwer, "Design Parameters Estimations for Bubble Column Reactors," *AIChE J.*, **28**, 353 (1982).
Shnip, A. I., R. V. Kolhatkar, D. Swamy, and J. B. Joshi, "Criteria for the Transition from the Homogeneous to the Heterogeneous

Regime in Two-Dimensional Bubble Column Reactors," *Int. J. Multiphase Flow*, **18**, 705 (1992).
Tarmy, B. L., M. Chang, C. A. Coulaloglou, and P. R. Ponzi, "Hydrodynamic Characteristics of Three-Phase Reactors," *The Chemical Engineer*, **407**, 18 (1984).
Wendt, R., A. Steiff, and P. M. Weinspach, "Liquid Phase Dispersion in Bubble Columns," *Ger. Chem. Eng.*, **7**, 267 (1984).
Wilkinson, P. M., H. Haringa, and F. P. A. Stokman, "Liquid Mixing in a Bubble Column Under Pressure," *Chem. Eng. Sci.*, **48**, 1785 (1993).
Yang, G. Q., X. Luo, R. Lau, and L. S. Fan, "Heat-Transfer Characteristics in Slurry Bubble Columns at Elevated Pressures and Temperatures," *Ind. Eng. Chem. Res.*, **39**, 2568 (2000).
Zahradnik, J., M. Fialova, M. Ruzicka, J. Drahos, F. Kastanek, and N. H. Thomas, "Duality of the Gas-Liquid Flow Regimes in Bubble Column Reactors," *Chem. Eng. Sci.*, **52**, 3811 (1997).

Manuscript received Aug. 30, 2001, revision received May 22, 2002.